Journal of Materials Chemistry C

Magnetoelectric effect in a cubic ferrimagnetic spinel LiFe5O8 with high coupling temperature

Journal:	*Journal of Materials Chemistry C*
Manuscript ID	TC-ART-11-2018-005615.R2
Article Type:	Paper
Date Submitted by the Author:	07-Jan-2019
Complete List of Authors:	Liu, Run; Sichuan Normal University, College of Chemistry and Materials Science Pan, Linlin; Sichuan Normal University, College of Chemistry and Materials Science Peng, Silu; Sichuan Normal University, College of Chemistry and Materials Science Chengdu Qin, Lili; Sichuan Normal University, College of Chemistry and Materials Science Bi, Jian; Sichuan Normal University, College of Chemistry and Materials Science Wu, Jiangtao; Sichuan Normal University, Chemistry and Materials Science Wu, Hua; Donghua University, Applied Physics; Simon Fraser University, Chemistry Ye, Zuo-Guang; Simon Fraser University, Chemistry

Magnetoelectric effect in a cubic ferrimagnetic spinel $LiFe_5O_8$ with high coupling temperature

Run Liu,[1] Linlin Pan,[1] Silu Peng,[1] Lili Qin,[1] Jian Bi,[1] Jiangtao Wu,[1]† Hua Wu, [2,3]† and Zuo-Guang Ye[3]†

[1.] College of Chemistry and Materials Science, Sichuan Normal University, Chengdu 610068, China

[2.] Department of Applied Physics, Donghua University, 201620 Shanghai, China

[3.] Department of Chemistry & 4D LABS, Simon Fraser University, Burnaby, BC, V5A 1S6, Canada.

† Corresponding authors. E-mails: Jiangtao Wu (jtwu@sicnu.edu.cn), Hua Wu (wuhua@dhu.edu.cn) and Zuo-Guang Ye (zye@sfu.ca)

Abstract: We report an effective magnetoelectric (ME) coupling phenomenon in cubic ferrimagnetic spinel $LiFe_5O_8$, with the command of its polarization by an applied magnetic field. A hysteretic response between magnetic field and electric polarization was observed. It is found that $LiFe_5O_8$ exhibits ME coupling that becomes significant at 250 K and increases with decreasing temperature. In contrast to many other spinel oxides that were reported to exhibit ME effect at very low temperatures (typically below 30 K), the bulk $LiFe_5O_8$ demonstrates a ME coefficient of 2 $mV \cdot Oe^{-1} \cdot cm^{-1}$ at 120 K. This material exhibits the highest ME coupling temperature among the magnetoelectric spinel and related materials so far reported. This ME effect is attributed to the ordered arrangement of magnetic ions (Fe^{3+}) which are located in a noncentrosymmetric coordination environment. Our result provides a

new venue to search for single-phase magnetoelectric materials with high coupling temperatures that could be used in potential technological applications.

Keywords: $LiFe_5O_8$, spinel magnetoelectrics, magnetoelectric effect

1 INTRODUCTION

Magnetoelectric (ME) materials that exhibit a cross coupling between magnetic and electric order parameters have gained increasing interest due to their significant potential for new-generation electronic and spintronic devices [1-6]. Materials with a spinel structure and general formula of AB_2O_4 (where A and B are metal ions, such as Co^{2+}, Zn^{2+}, Fe^{3+}, and Cr^{3+}) have become promising ME materials due to their widely tunable crystal structure and intricate magnetic/electric properties. Spinels typically have a high permeability value with high resistivity that prevents the eddy current energy losses, making them a good candidate for magnetoelectrics. However, at present, only a few spinel compounds were reported to exhibit ME effect which only occurred at very low temperatures, such as $ZnCr_2Se_4$ (20 K)[7] , $CoCr_2O_4$ (27 K),[8] $CoAl_2O_4$ (3 K),[9] and $MnGa_2O_4$ (20 K)[10]. Therefore, developing higher-temperature and ideally room-temperature ME materials with spinel structure is a challenging task which may lead to technological applications of spinel ME materials in advanced devices and help better understand the microscopic mechanisms underlying the structure-ME property relationship.

This work we explore a material from the family of spinel oxides, $LiFe_5O_8$, that exhibits effective ME effect at relatively high temperatures (120 - 300 K). $LiFe_5O_8$ crystallizes in a B-site-ordered spinel structure with a cubic symmetry of $P4_332$ at

room temperature.[11] Fig. 1(a) shows the schematic of the crystal structure in which all Li^+ ions occupy the octahedral B-sites, whereas Fe^{3+} ions in high-spin state (S = 5/2) occupy the slightly distorted octahedral B-sites (Fe_2) and tetrahedral A-sites (Fe_1) with a 3:2 ratio. We consider $LiFe_5O_8$ to be a potential ME material at high temperatures based on the following reasoning. Firstly, according to Rado's calculation,[12] a magnetic field dependence of the magnetically induced electric polarization should exist in $LiFe_5O_8$, and moreover, Gridnev provided some indirect evidence of the ME effect in a $LiFe_5O_8$ single crystal at low temperature.[13] Secondly, $LiFe_5O_8$ crystallizes in the $P4_332$ space group, in which the first and second order ME effects are allowed in principle.[14] Finally, $LiFe_5O_8$ possesses a large magnetization, which favors a strong ME coupling effect.[15] All of these features render $LiFe_5O_8$ a possible candidate as ME material near room temperature.

In this work, bulk cubic spinel $LiFe_5O_8$ was synthesized and its ME property was then systematically studied. It is found that bulk $LiFe_5O_8$ exhibits a hysteretic ME signal at room temperature (300 K). The ME properties of $LiFe_5O_8$ could be attributed to the ordered arrangement of Fe^{3+} ions located in a noncentrosymmetric coordination environment along the [110] direction;[16] this interpretation was supported by previous theoretical studies[10, 17]. Our results demonstrate that spinel $LiFe_5O_8$ exhibits the ME effect at relatively high temperatures and provide a new pathway to search for new room temperature ME materials.

2 EXPERIMENTAL

$LiFe_5O_8$ powders were prepared by solid-state reaction method. In brief, α-Fe_2O_3

and Li_2CO_3 were milled and heated at 800 °C for 5 h (α-Fe_2O_3 and Li_2CO_3 were dried first at 200 °C for 7 h). The as-prepared $LiFe_5O_8$ powders were ground into fine powders and pressed into pellets with 6 wt.% polyvinyl alcohol as binding agent. The pellets were sintered in a furnace at 950 °C for 5 h in ambient atmosphere to form dense ceramics. Both surfaces of the sintered ceramics were finely polished and coated with silver paste electrodes.

X-ray powder diffraction (XRD) patterns were obtained using a SmartLab diffractometer with Cu K_α radiation (Rigaku, Japan). Magnetic properties were measured using a vibrating sample magnetometer (VersaLab and PPMS, Quantum Design, Inc., USA). Magnetodielectric (magnetocapacitance) effect is commonly considered to be a kind of ME behavior, which can also be exemplified by the combination of magnetoresistance and the Maxwell-Wagner effect [18]. However, these effects are not from true ME coupling phenomena. In this work, the ME properties were characterized by measuring the direct ME voltage signal induced by the magnetic field, i.e., $E(H_{ac})^2$. The ME effect can be quantitatively described by the ME coefficient $\alpha_E = \Delta E/\Delta H_{ac}$. This parameter represents the variation in the ME voltage signal (ΔE) under a small *ac* magnetic field ΔH_{ac} (1 Oe, 100 kHz) superimposed on a *dc* magnetic field H_{dc} (-20 to 20 kOe) with the dc and ac magnetic fields being perpendicular to the surface of the sample. The induced ME voltage signal ΔE and phase difference were measured and recorded by a lock-in amplifier locked at the H_{ac} excitation frequency and phase (SR830, SRS Inc., USA). The induced Faraday electromotive force was eliminated from the raw data. Typically, the induced Faraday

electromotive force is about 1 μV (whereas $\alpha_E > 15$ μV).

3 RESULTS AND DISCUSSION

Room-temperature XRD analysis was performed to study the crystal structures of $LiFe_5O_8$. The XRD pattern in Fig. 1(b) can be indexed to a cubic structure with the noncentrosymmetric space group of $P4_332$. The XRD data at room temperature were refined by the Rietveld method using GSAS software to confirm the crystal structure and obtain the atom positions of $LiFe_5O_8$ [Fig. 1(c)]. The Rietveld refinement results (red line) fit well the observed XRD data (black cross), and confirmed that $LiFe_5O_8$ possesses a cubic spinel structure with lattice parameters $a = b = c = 8.3237$ Å. The statistical parameters (χ^2, R_p, and R_{wp}) are 0.663, 2.35%, and 1.83%, respectively. The low values of reliability factors indicate the high accuracy of the structural analysis. Table I lists the parameters of atomic coordinates, where *x/a*, *y/b*, and *z/c* represent the spatial coordinate axis and $O_1^{2-}$and O_2^{2-} refer to the oxygen ions connecting two Fe^{3+} ions and connecting Li^+ and Fe^{3+} ions, respectively. Our results show that the Fe^{3+} ions of this spinel oxide occupy both the slightly distorted octahedral B-site and the tetrahedral A-site, leading to their displacements from the center of the octahedron and tetrahedron. This finding is in accordance with the published results [11, 16].

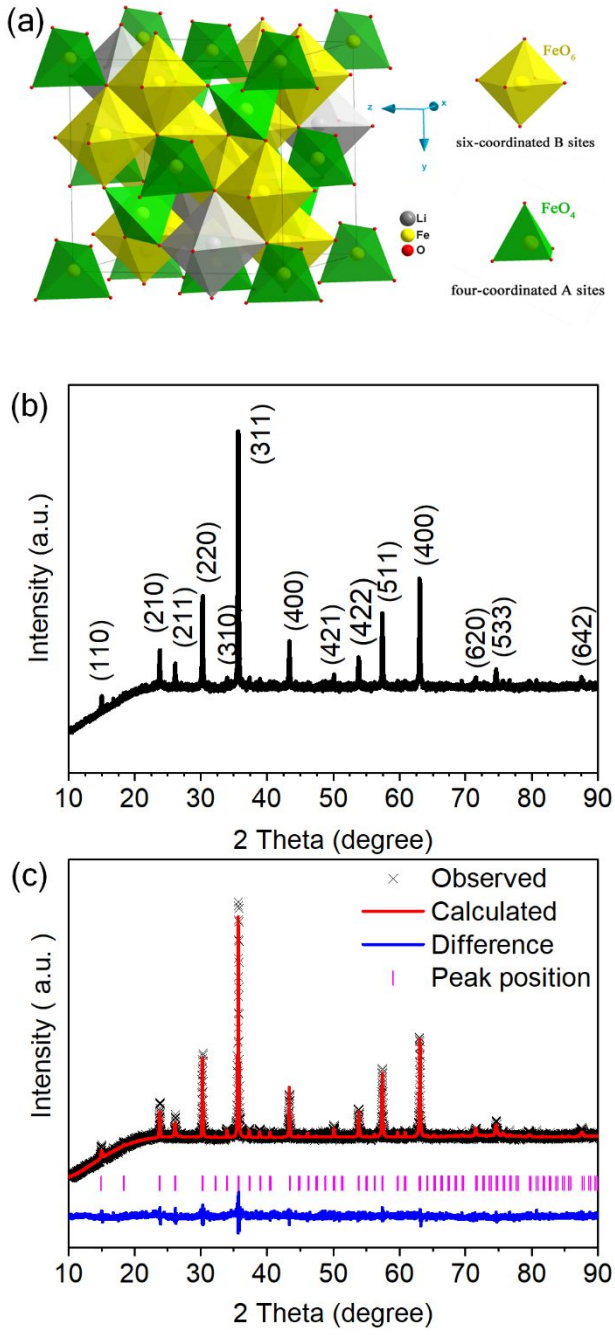

FIG. 1. (a) Schematic of the crystal structure of $LiFe_5O_8$. (b) XRD patterns of $LiFe_5O_8$ samples. (c) Observed XRD data (black cross), calculated data (red line), and difference (blue line) between the observed data and refinement results of $LiFe_5O_8$. The pink lines refer to the position of the Bragg's reflection peak of this compound.

TABLE I. Refined structural positions of cations/anions in $LiFe_5O_8$

Ions	Wyckoff position	*x/a*	*y/b*	*z/c*
Li^+	4b	0.6250(0)	0.6250(0)	0.6250(0)
Fe_1^{3+}	8c	0.9981(4)	0.9981(4)	0.9981(4)
Fe_2^{3+}	12d	0.1250(0)	0.3681(4)	0.8819(4)
O_1^{2-}	8c	0.3825(15)	0.3825(15)	0.3825(15)
O_2^{2-}	24e	0.1233(10)	0.1318(10)	0.3725(10)

Fig. 2(a) shows the magnetization-magnetic field (*M-H*) relation measured at the temperatures of at 300, 250, 200, 150 and 120 K. As shown in Figure 2 (a), $LiFe_5O_8$ displays similar slim magnetic hysteresis loops at these temperatures. The coercive field H_c is 100 Oe and the remnant magnetization is about 9 emu/g, indicating that $LiFe_5O_8$ is magnetically soft. The values of the saturation magnetization M_s are found to be 63.6, 63.2, 62.2, 60.3 and 58.9 emu/g at 120, 150, 200, 250, and 300 K, respectively, as shown in Figure 2 (b). The magnetism originates from the antiparallel spin alignment between Fe_2 and Fe_1.[15] The strong and intrinsic magnetic interaction in $LiFe_5O_8$ at 300 K is favorable for developing ME effects.[19] Fig. 2(c) exhibit the zero-field-cooled (ZFC) and field-cooled (FC) magnetization behavior of $LiFe_5O_8$ at the field of 10, 100 and 1000 Oe between 300 and 10 K. It can be seen that under the fields of 10 and 100 Oe, the ZFC and FC curves start to split at 170 and 230 K, respectively, and the difference in the magnetic moments between ZFC and FC increases as the temperature decreases, more significantly at lower field. At 10 K, the

relative difference in the magnetic moments reaches 21 % and 3 % under 10 and 100 Oe, respectively. When the external field increases to 1000 Oe, the splitting of the ZFC/FC curves can be observed at about 210 K, with the difference in magnetic moments increasing upon cooling to 120 K and then decreasing upon further cooling before reaching zero at 10 K. These variations of magnetization upon ZFC and FC at different fields represent the typical behavior of a spin glass system [20, 21], which can be attributed to the competition between the glassy spin interactions and the Zeeman effect. In a spin glass system, the magnetization first increases upon cooling until the random interactions cause the spins to freeze out in random directions, resulting in a decrease in magnetization upon further cooling. The temperature at which the magnetization starts to decrease under weak fields (10 Oe in this wrok) is typically called the "blocking temperature". Accordingly, the blocking temperature for $LiFe_5O_8$ is found to be about 120 K at which the ZFC curve began to decrease because of the spin freezing. On the other hand, an external magnetic field tends to align the spins parallel to the field, giving rise an increasing magnetization. Therefore, the ZFC/FC curves split normally. A strong enough magnetic field can gradually destroy the spin glass state, so the ZFC/FC curves tend to overlap with each other with a smaller split.

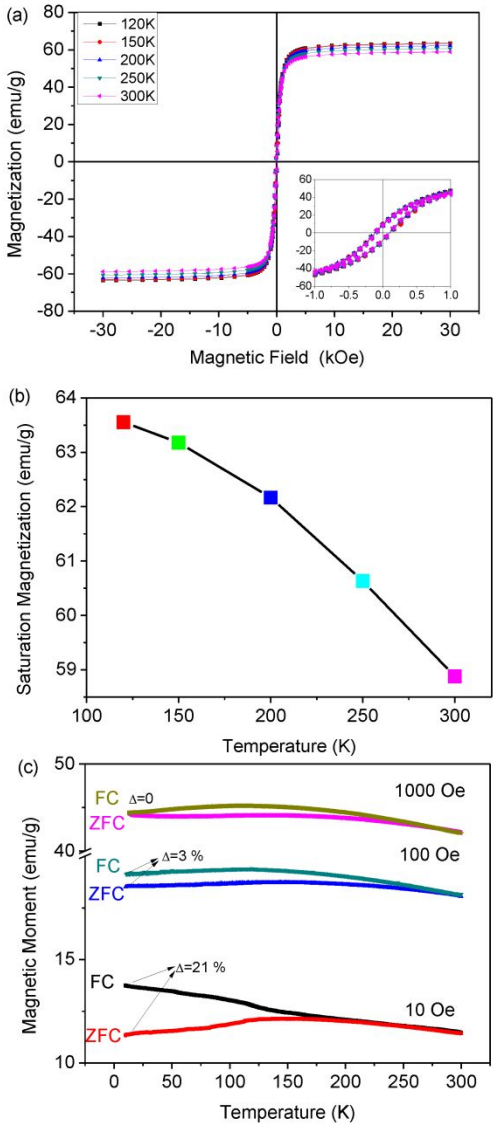

FIG. 2 (a) Magnetic hysteresis loops for $LiFe_5O_8$ measured at 120, 150, 200, 250 and 300 K. Inset shows the hysteretic behavior of magnetization between -1 kOe and 1 kOe. (b) Variation of the saturation magnetization with temperature. (c) Variations of the ZFC and FC magnetization measured between 300 and 10 K at a field of 10, 100 and 1000 Oe.

The ME effect of $LiFe_5O_8$ was measured in the form of ME coefficient (α_E). Figs. 3(a) and (b) display the variation of α_E as a function of magnetic field (α_E-H) at various temperatures. Obviously, α_E exhibits a significant dependence on external

magnetic field upon cooling (from 300 to 120 K), thereby indicating a coupling between the magnetic and electrical subsystems. The variation of α_E as a function of magnetic field between 300 and 120 K looks similar to the *M*-*H* loop, demonstrating a sharp increase when the field varies from -10 kOe to 10 kOe and a sharp decrease when the field changes from 10 kOe to -10 kOe. It reaches saturation at the fields of 10 kOe to 20 kOe (and -10 kOe to -20 kOe). The magnetization reaches saturation at about 4 kOe at various temperatures between 300 and 120 K (Fig 4 a), while the ME coupling curves reach "saturation" at the fields of 10 - 15 kOe at temperatures below 250 K. At 300 K, the ME coefficient seems to increase with increasing magnetic field up to 20 kOe. It is known that in artificial (composite) ME materials, for example, the PZT/Co composite, the saturation magnetization field typically equals the saturation ME field because the ME effect mainly originates from the interface strain via magnetostricive effect which in turn generates electric polarization through piezoelectric effect. For single-phase ME materials like $LiFe_5O_8$, however, the dependences of the magnetization and ME coefficient on magnetic field and their respective saturation fields are not necessarily the same because the ME effect results from an intrinsic mechanism through the interaction of magnetic field with the spins of the ordered magnetic ions (Fe^{3+}) located in a noncentrosymmetric coordination environment, which in turn causes the changes in electric polarization. In addition, the competition between the two crystalline anisotropies (tetrahedral and octahedral sites) and the shape anisotropies may result in the rotation of the easy direction of magnetization under an increasing magnetic field, causing the ME effect to saturate at

a higher field than the saturating field of the M-H relation. The difference in the magnetization saturation field and ME saturation field is commonly found in other single-phase materials. For example, in Dy-doped $BiFeO_3$ ($Bi_{0.88}Dy_{0.12}Fe_{0.97}Ti_{0.03}O_3$), the saturation magnetization field is 25 Oe, while the saturation ME field is about 100 Oe[2] and in Sm-doped $BiFeO_3$, these two fields 20 kOe and less than 1 kOe, respectively[22]. The nearly linear increase of ME coefficient with magnetic field at 300 K may be due to its weak ME effect, like in some other magnetoelectrics which do not show any "saturation" in the ME effect and their ME coefficient increases linearly with magnetic field, such as $Bi_{0.68}La_{0.32}Fe_{0.655}Mn_{0.025}Ti_{0.32}O_3$[23] and $Bi_{0.87}La_{0.05}Tb_{0.08}FeO_3$[24].

Fig. 3(c) depicts the temperature dependence of α_E measured at the magnetic field of 15 kOe. α_E increases with the decrease in temperature and its value reaches 2 $mV \cdot Oe^{-1} \cdot cm^{-1}$ at 120 K (0.11 ps/m), which indicates an significant ME effect at a relatively high coupling temperature. Figure 3(d) shows the temperature - electricity curve form 300 K to 200 K. It can be seen from Figure 3(d) that the resistivity at 300 K is in the order of 10^5 Ohm.m and it increases with the decrease of temperature, first slowly below room temperature and then sharply below 250 K. This result corroborates our statement that spinels, as represented here by $LiFe_5O_8$, exhibit high resistivity, making them good candidates as ME materials. With the decrease of temperature, ρ(T) shows a slow rise near room temperature (270-300 K) and followed by a steep increase below ~250 K, suggests that the resistivity is substantially enhanced with the decrease of temperature. It is interesting to note that the

temperature dependences of the ME coefficient and resistivity show the same trend: both decreasing sharply with the increase of temperature. This suggests that the decrease of the measured ME coefficient values (α_E) at temperatures above 200 K may be partially caused by the loss of magnetically induced charge (polarization) due to a higher conductivity. So, the decreasing values of the measured α_E at temperatures above 120 K may be caused by two effects: i) the weakening of ME coupling and ii) the loss of magnetically induced charge (polarization) due to higher conductivity at high temperatures.

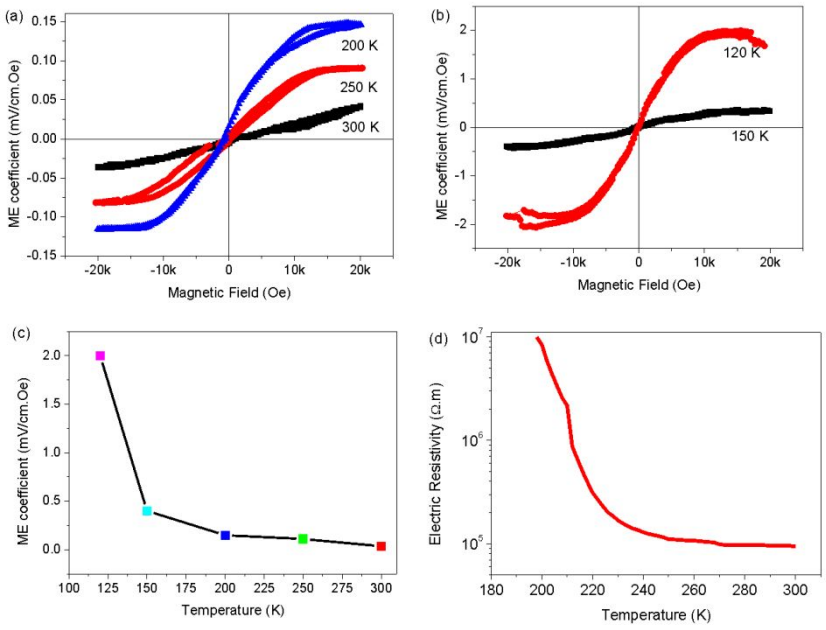

FIG. 3. (a), (b)Variation of ME coefficient as a function of the external magnetic field measured at various temperatures for $LiFe_5O_8$ and (c) temperature dependence of the maximum value of ME coefficient. (d). Temperature dependence of *dc* electric resistivity.

Although some spinels were reported to exhibit magnetoelectric effects, such as

$CoCr_2O_4$ (26 K),[25] $MnCr_2O_4$ (17 K),[26] Mn_3O_4 (40 K),[27] CdV_2O_4 (33 K),[28] $CdCr_2S_4$(75 K)[29], only the ME coefficients of a few compounds have been measured. Figure 4 presents the reported ME coefficients of spinel compounds together with the value of $LiFe_5O_8$ measured in this work. It can be clearly seen that, compared with the spinel materials that display ME effect at low temperatures, including $CoAl_2O_4$ (calculated),[9] Fe_3O_4 nanoparticles,[30] $ZnGr_2Se_4$,[7] Co_3O_4 and $MnAl_2O_4$ (calculated),[10] the bulk $LiFe_5O_8$ exhibits a decent ME effect at a much higher coupling temperature. Note that although Co_3O_4 and $CoAl_2O_4$ reportedly exhibted high ME effect, their α_E values were calculated only and have not been measured experimentally. Moreover, the extrime toxicity of Co element and the low coupling temperatures make them unsuitable for ME applications.

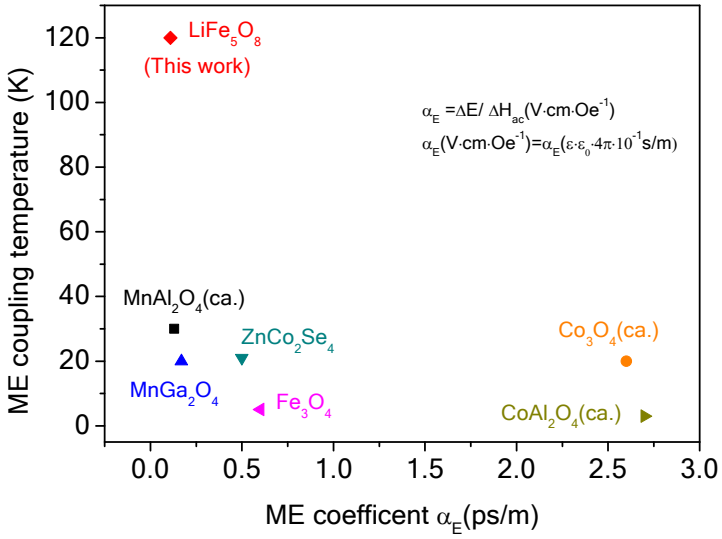

FIG. 4. Ordering temperature and ME coefficient (α_E) of reported spinel magnetoelectrics and $LiFe_5O_8$ of this work. Note that the α_E values of $CoAl_2O_4$, Co_3O_4 and $MnAl_2O_4$ were calculated values only.

We believe that the aforementioned ME coupling in $LiFe_5O_8$ arises the noncentrosymmetric crystal structure and the ordered arrangement of Fe^{3+} ions. From the view of the crystal symmetry of $P4_332$, $LiFe_5O_8$ has a spinel structure with cations ordering in the octahedral position in the [110] direction with every cubic unit cell containing three Fe^{3+} ions ($Fe_{2,1}$, $Fe_{2,2}$, and $Fe_{2,3}$) and one Li^+ ion in the (110) plane [Fig. 5(b)]. In accordance with the crystal chemistry, the Fe^{3+} ion occupying the slightly distorted B-sites exhibits a nonzero local electric polarization P_i, which is represented by a gray arrow in Fig. 5(a), through the two-fold rotational axis symmetry (C_2).[31] Thereby, the three Fe^{3+} ions in the (110) plane exhibit electric dipoles $\vec{P}_{1,2}$ $\vec{P}_{2,2}$ and $\vec{P}_{2,3}$(gray arrows) with equal magnitude and different directions along $[\bar{1}0\bar{1}]$, $[\bar{1}\bar{1}0]$, and $[0\bar{1}1]$, respectively [Fig. 5(b)]. The electric polarization of the unit cell arises from the nonzero total dipolar moment $\vec{P}_t$, which can be expressed as $\vec{P}_t = \vec{P}_{2,1} + \vec{P}_{2,2} + \vec{P}_{2,3}$, and is along the $[\bar{1}\bar{1}0]$ direction and perpendicular to the (110) plane [Fig. 5(b)]. As for the magnetic interaction, Fe^{3+} has electron configuration $(t_{2g})^3(e_g)^2$ that provides five unpaired electrons at the high-spin state, constituting the unquenched orbital spin momentum. Herein, the spin $\vec{S}$ of Fe^{3+} ions occupying the octahedral site will modify the electric polarization due to spin–orbital coupling, which results in the spin dependence of the electric polarization and the coupling between polarization and magnetization, giving rise to the ME effects.

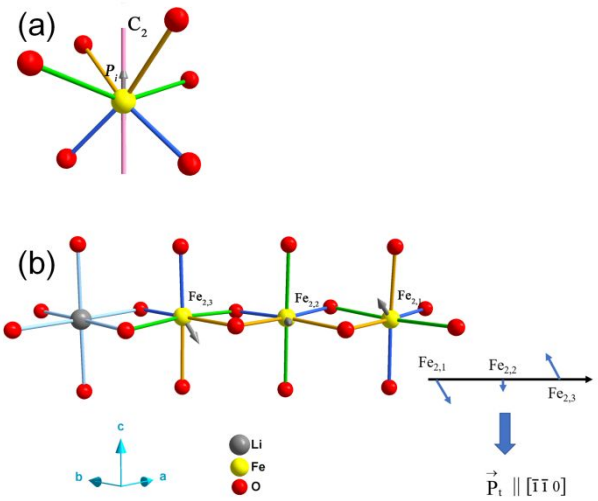

FIG. 5. (a) Fe^{3+} on a site of two-fold (C_2) symmetry formed by a distorted oxygen octahedron. The rotational C_2 symmetry axis is indicated (Note: the same color of bond represents the same bond length). (b) Three Fe^{3+} ions in the unit cell with their respective electric dipole moments (gray arrows).

4 CONCLUSIONS

In this study, the ME effect of the cubic spinel $LiFe_5O_8$ was investigated and the ME coefficient was measured through the command of polarization by an applied dc magnetic field (H_{dc}) between 120 and 300 K using a lock-in amplifier. It is found that $LiFe_5O_8$ exhibits ME coupling that becomes significant at 250 K and increases with decreasing temperature. In contrast to many other spinel oxides that were reported to exhibit ME effect at very low temperatures (typically below 30 K), the bulk $LiFe_5O_8$ demonstrates a decent ME effect at much higher ordering temperatures with the maximum ME coefficient reaching 2 $mV \cdot Oe^{-1} \cdot cm^{-1}$ at a temperature as high as 120 K. The Fe^{3+} ions at a site of noncentrosymmetric coordination and the cation ordering are believed to give rise to the coupling between the local electric polarization and the

spin via spin–orbital interaction, leading to the observed magnetoelectricity in $LiFe_5O_8$.

The ME effect in $LiFe_5O_8$ could be further enhanced by improving the material quality through chemical modification and/or physical means, such as annealing, doping, single crystal growth, thin film deposition, etc. This work reveals that $LiFe_5O_8$ as a prototype of spinel materials with high magnetic phase transition temperature and noncentrosymmetric structure possesses the possibility to become a promising material with significant ME coupling at relatively high temperatures, potentially useful for new-generation electronic and spintronic device. It also provides insights into the microscopic mechanisms of ME effect in spinel which will be helpful in designing new single-phase ME materials.

Acknowledgments

The authors gratefully acknowledge Jian Zhuang, Xi'an Jiaotong Unversity for measuring the ZFC/FC properties of LFO. This work was supported by the National Natural Science Foundation of China (Grant No. 21401133), the Natural Sciences and Engineering Research Council of Canada (NSERC, Grant No. 203773) and the United States Office of Naval Research (ONR Grants No. N00014-12-1-1045 and N00014-16-1-3106).

References

1. T. Amrillah, Y. Bitla, K. Shin, T. Yang, Y. H. Hsieh, Y. Y. Chiou, H. J. Liu, T. H. Do, D. Su, Y. C. Chen, S. U. Jen, L. Q. Chen, K. H. Kim, J. Y. Juang and Y. H. Chu, *ACS Nano*, 2017, **11**, 6122-6130.
2. L. Pan, Q. Yuan, Z. Liao, L. Qin, J. Bi, D. Gao, J. Wu, H. Wu and Z.-G. Ye, *J. Alloys Compd.*, 2018, **762**, 184-189.
3. J. A. Mundy, C. M. Brooks, M. E. Holtz, J. A. Moyer, H. Das, A. F. Rebola, J. T. Heron, J. D. Clarkson, S. M. Disseler, Z. Liu, A. Farhan, R. Held, R. Hovden, E. Padgett, Q. Mao, H. Paik, R. Misra, L. F. Kourkoutis, E. Arenholz, A. Scholl, J. A. Borchers, W. D. Ratcliff, R. Ramesh, C. J. Fennie, P. Schiffer, D. A. Muller and D. G. Schlom, *Nature*, 2016, **537**, 523-527.
4. H. Xi, X. Qian, M. C. Lu, L. Mei, S. Rupprecht, Q. X. Yang and Q. M. Zhang, *Sci. Rep.*, 2016, **6**,

29740.
5. J. Wu, Z. Shi, J. Xu, N. Li, Z. Zheng, H. Geng, Z. Xie and L. Zheng, *Appl. Phys. Lett.*, 2012, **101**, 122903.
6. M. M. Sang-Wook Cheong, *Nat. Mater.*, 2007, **6**, 13-20.
7. H. Murakawa, Y. Onose, K. Ohgushi, S. Ishiwata and Y. Tokura, *J. Phys. Sco. Jpn*, 2008, **77**, 043709.
8. Y. Yamasaki, S. Miyasaka, Y. Kaneko, J. P. He, T. Arima and Y. Tokura, *Phys. Rev. Lett.*, 2006, **96**, 207204.
9. S. Ghara, N. V. Ter-Oganessian and A. Sundaresan, *Phys. Rev. B*, 2017, **95**, 094404.
10. R. Saha, S. Ghara, E. Suard, D. H. Jang, K. H. Kim, N. V. Ter-Oganessian and A. Sundaresan, *Phys. Rev. B*, 2016, **94**, 014428.
11. P. B. Braun, *Nature*, 1952, **170**, 1123–1123.
12. G. T. Rado, J. M. Ferrari and J. P. Remeika, *J. Appl. Phys.*, 1978, **49**, 1953.
13. V. N. Gridnev, B. B. Krichevtsov, V. V. Pavlov and R. V. Pisarev, *J. Exp. Thero. Phys.*, 1997, **65**, 68-73.
14. M. Mercier, G. Velleaud and J. Puvinel, *Physica*, 1977, 86-88.
15. R. Zhang, M. Liu, L. Lu, S.-B. Mi and H. Wang, *J. Mater. Chem. C*, 2015, **3**, 5598-5602.
16. J. L. Dormann, A. Tomas and M. Nogues, *Phys. Stat. Sol. (A)*, 1983, **77**, 611–618.
17. V. P. Sakhnenko and N. V. Ter-Oganessian, *J. Phys.: Condens. Matter*, 2012, **24**, 266002.
18. G. Catalan, *Appl. Phys. Lett.*, 2006, **88**, 102902.
19. H. Wu and W. Z. Shen, *Solid State Comm.*, 2005, **133**, 487-491.
20. W. Luo, S. R. Nagel, T. F. Rosenbaum and R. E. Rosensweig, *Phys. Rev. Lett.*, 1991, **67**, 2721-2724.
21. K. Binder, *Rev. Mod. Phys.*, 1986, **58**, 801-976.
22. V. Sreenivas Puli, D. Kumar Pradhan, S. Gollapudi, I. Coondoo, N. Panwar, S. Adireddy, D. B. Chrisey and R. S. Katiyar, *J. Magn. Magn. Mater*, 2014, **369**, 9-13.
23. C. M. Fernandez-Posada, A. Castro, J. M. Kiat, F. Porcher, O. Pena, M. Alguero and H. Amorin, *Nat. Commun.*, 2016, **7**, 12772.
24. Q. H. Jiang, J. Ma, Y. H. Lin, C.-W. Nan, Z. Shi and Z. J. Shen, *Appl. Phys. Lett.*, 2007, **91**, 022914.
25. S. Tiwari and D. Sa, *J. Phys.: Condens. Matter*, 2010, **22**, 225903.
26. N. Mufti, G. R. Blake and T. T. M. Palstra, *J. Magn. Magn. Mater*, 2009, **321**, 1767-1769.
27. T. Suzuki and T. Katsufuji, *Journal of Physics: Conference Series*, 2009, **150**, 042195.
28. G. Giovannetti, A. Stroppa, S. Picozzi, D. Baldomir, V. Pardo, S. Blanco-Canosa, F. Rivadulla, S. Jodlauk, D. Niermann, J. Rohrkamp, T. Lorenz, S. Streltsov, D. I. Khomskii and J. Hemberger, *Phys. Rev. B*, 2011, **83**, 060402(R).
29. P. L. J. Hemberger, R. Fichtl, H.-A. Krug von Nidda, and V. T. A. Loidl, *Nature*, 2005, **434**, 364-367.
30. K. Yoo, B. G. Jeon, S. H. Chun, D. R. Patil, Y. J. Lim, S. H. Noh, J. Gil, J. Cheon and K. H. Kim, *Nano Lett.*, 2016, **16**, 7408-7413.
31. S.J.Marin, M.O'Keeffe and D.E.Partin, *J. Solid State Chem.*, 1994, **113**, 413-419.